Molecular Orbital Studies of Titanium Nitride Chemical Vapor Deposition: Imido Dimer Formation and Elimination Reactions

Jason B. Cross, Stanley M. Smith, and H. Bernhard Schlegel*

Department of Chemistry, Wayne State University, Detroit, Michigan 48202

Received October 20, 2000. Revised Manuscript Received January 18, 2001

The dimerization of $Ti(NH_2)_2NH$ has been used as a model for the generalized oligomerization of $Ti(NR_2)_2NH$ in the chemical vapor deposition (CVD) of titanium nitride films. This study uses molecular orbital methods (specifically the B3LYP/6-311G(d) level of theory) to examine the dimerization process and the subsequent elimination of N_2H_4 from this model compound by two different reaction paths. There is no transition structure for the formation of the dimer from two $Ti(NH_2)_2NH$ molecules, and this reaction is barrierless. The binding energies of the singlet and triplet dimer complexes are 99.1 and 49.0 kcal/mol, respectively. Both N_2H_4 elimination pathways are endothermic, and enthalpies of reaction are 26.2 and 17.7 kcal/mol for the singlet and triplet pathways, respectively. In both pathways, there is a crossing from the singlet to triplet surface prior to the N_2H_4 elimination transition state. Structures on a reaction path for the exchange of amido and imido ligands in the ring of the dimer complex were also found. This pathway could lead to the formation of higher oligomers.

Introduction

Titanium nitride thin films have a number of desirable properties for commercial and industrial applications. Such characteristics include extreme hardness, high chemical resistivity, excellent electrical conductivity, and optical properties similar to those of gold. These qualities of titanium nitride films make them ideal for applications such as wear-resistant coatings for tools, barrier materials, and conductive coatings for microelectronics, solar coatings for glass, and decorative coatings.[1−4]

For semiconductor applications, chemical vapor deposition (CVD) is preferred over physical deposition when preparing thin films, since submicron devices require high-quality conformal coatings.[2] A number of preparation methods for Ti−N thin films have been developed,[5−12] but many of these are unsuitable due to the high temperatures required. At high temperatures (900−1000 °C), high-quality Ti−N films can be deposited using $TiCl_4$, N_2, and H_2.[6,7] At lower temperatures (500−700 °C) with ammonia as a nitrogen source, films can be deposited by the following process:[8]

$$TiCl_4 + {}^4/_3NH_3 \rightarrow TiN + 4HCl + {}^1/_6N_2 \qquad (1)$$

However, even lower temperatures are preferred for semiconductor applications (300−400 °C). At these temperatures, films made using $TiCl_4$ as a precursor contain a mixture of TiN and TiNCl.[9] The use of Ti(IV) amido precursors, $Ti(NR_2)_4$, can avoid the chlorine impurities in these films but introduces contamination from titanium carbide and organic carbon.[10,11,13,14] Experimental evidence collected by Dubois[5,15] has implicated Ti−N−C metallocycles as the source of the carbon contamination. These impurities can be eliminated through the use of excess ammonia in the CVD process, which results in high-quality films at the low temperatures required by the semiconductor industry:[12,16,17]

$$Ti(NR_2)_4 + \text{excess } NH_3 \rightarrow TiN + \text{volatile organics} \qquad (2)$$

Low-pressure CVD of Ti−N films occurs almost exclusively at the surface.[18] However, in atmospheric pressure Ti−N CVD, gas-phase reactions are key ele-

(1) Buhl, R.; Pulker, H. K.; Moll, E. *Thin Solid Films* **1981**, *80*, 265.
(2) Pintchovski, F.; Travis, E. *Mater. Res. Soc. Symp. Proc.* **1992**, *260*, 777.
(3) Travis, E. O.; Fiordalice, R. W. *Thin Solid Films* **1993**, *236*, 325.
(4) Erola, M.; Keinonen, J.; Anttila, A.; Koskinen, J. *Solar Energy Mater.* **1985**, *12*.
(5) Dubois, L. H. *Polyhedron* **1994**, *13*, 1329.
(6) Hoffman, D. M. *Polyhedron* **1994**, *13*, 1169.
(7) Schintlmeister, W.; Pacher, O.; Pfaffinger, K.; Raine, T. *J. Electrochem. Soc.* **1976**, *123*, 924.
(8) Kurtz, S. R.; Gordon, R. G. *Thin Solid Flims* **1986**, *140*, 277.
(9) Hegde, R. I.; Fiordalice, R. W.; Tobin, P. J. *Appl. Phys. Lett.* **1993**, *62*, 2326.
(10) Fix, R. M.; Gordon, R. G.; Hoffman, D. M. *Chem. Mater.* **1990**, *2*, 235.
(11) Fix, R. M.; Gordon, R. G.; Hoffman, D. M. *Mater. Res. Soc. Symp. Proc.* **1990**, *168*, 357.
(12) Fix, R.; Gordon, R. G.; Hoffman, D. M. *Chem. Mater.* **1991**, *3*, 1138.
(13) Sugiyama, K.; Pac, S.; Takahashi, Y.; Motojima, S. *J. Electrochem. Soc.* **1975**, *122*, 614.
(14) Fix, R. M.; Gordon, R. G.; Hoffman, D. M. *J. Am. Chem. Soc.* **1990**, *112*, 7833.
(15) Dubois, L. H.; Zegarski, B. R.; Girolami, G. S. *J. Electrochem. Soc.* **1992**, *139*, 3603.
(16) Musher, J. N.; Gordon, R. G. *J. Electrochem. Soc.* **1996**, *143*, 736.
(17) Musher, J. N.; Gordon, R. G. *J. Mater. Res.* **1996**, *11*, 989.
(18) Truong, C. M.; Chen, P. J.; Corneille, J. S.; Oh, W. S.; Goodman, D. W. *J. Phys. Chem.* **1995**, *99*, 8831.

10.1021/cm000840c CCC: $20.00
Published on Web 02/17/2001

ments of the process.[6] The mechanism of the CVD process in the gas phase is quite complex, and a combination of experimental and computational work is beginning to elucidate the details of this process. Evaluation of the thermochemistry of potential intermediates in Ti−N CVD is an important step for understanding the overall mechanism, and we have calculated the gas phase heats of formation of $TiCl_m(NH_2)_n$ ($0 \le m + n \le 4$), $TiCl_m(NH_2)_nNH$ ($0 \le m + n \le 2$), and $TiCl_m(NH_2)_nN$ ($0 \le m + n \le 1$) at the G2 level of theory.[19] The results are in agreement with recent experimental values for $TiCl_n$,[20] and the theoretical bond dissociation energies should be accurate to ±2 kcal/mol. $TiCl_4$ and $TiCl_2(NH_2)_2$ readily form complexes with ammonia.[21−23] Siodmiak, Frenking, and Korkin[24] have studied ammonolysis of $TiCl_4$ using various levels of theory up to CCSD(T) with pseudopotentials and a split-valence basis set. The $TiCl_4 + NH_3$ binding energy has been calculated to be ca. 12−24 kcal/mol,[24,25] and replacement of Cl by NH_2 is computed to be endothermic by ca. 10−20 kcal/mol per Cl.[19,24] We also explored the complex formation, ligand exchange, and elimination reactions involving $TiCl_4$ and $Ti(NH_2)_4$ with NH_3.[26] At the MP2/6-311+G(3df,2p) level of theory the $Ti(NH_2)_4{\cdot}NH_3$ complex is bound by 7.9 kcal/mol, and the ligand exchange reaction has a barrier of 8.4 kcal/mol at the B3LYP/6-311+G(3df,2p) level of theory.[26] The barrier for formation of $Ti(NH_2)_2NH$ from $Ti(NH_2)_4$ is 33.5 kcal/mol, which is reduced by 10 kcal/mol when assisted by binding of an additional NH_3 (although in this case the free energy of the reaction increases by 10 kcal/mol).[26]

Since further elimination from the imido complexes studied in our previous paper seems unlikely due to thermodynamic considerations,[26] subsequent reactions leading to reduction of Ti(IV) in the gas phase to Ti(III) in the film must occur either on the surface or along another path available in the gas phase. Bond cleavage in the gas phase is unlikely, since the dissociation energies are quite high (75−120 kcal/mol calculated for Ti(IV) chloro, amido, imido, and nitrido compounds[19]). Dubois[5] has presented evidence that large oligomeric clusters with bridging imido groups form in the gas phase during Ti−N CVD. Other groups have synthesized titanium compounds containing a variety of bridging imido ligands.[27−29] Experimental evidence also suggests that imido compounds play a role as intermediates in Ti−N thin film growth.[30] Films made using the cyclic $[Ti(\mu\text{-N-}t\text{-Bu})(NMe_2)_2]_2$ imido precursor have chemical compositions very similar to those made using $Ti(NMe_2)_4$ and $Ti(NMe_2)_3(t\text{-Bu})$.[31] It is suspected that these oligomeric clusters are the species that stick to the surface and eventually form Ti−N.[5]

In this paper we continue to explore the gas-phase reaction pathways in Ti−N CVD using computational methods. In particular, we examine the dimerization of $Ti(NH_2)_2NH$ as a model for the oligomers suggested by Dubois[5] and the elimination pathways which lead to an oxidation state change from Ti(IV) to Ti(III) in the gas phase.

Method

Molecular orbital calculations were carried out using the GAUSSIAN 98[32] series of programs. Equilibrium geometries for complexes and transition states were optimized using the B3LYP hybrid density functional method[33−35] with the 6-311G(d) basis set.[36−40] For titanium, this corresponds to the 14s,9p,5d Wachters−Hay[38−40] basis set contracted to 9s,5p,3d and augmented with an f-type Gaussian shell with an exponent of 0.690. Since it was not clear at the outset whether a potential energy surface crossing would occur along the reaction paths studied, all structures were optimized as both singlets and triplets, using spin-unrestricted B3LYP calculations for the triplets. Vibrational frequencies and zero-point energies were computed at the B3LYP/6-311G(d) level of theory and were used without scaling since the B3LYP frequencies compare favorably with experimental values for a wide range of second and third period compounds.[41] Thermal and free energy corrections to the energies were calculated by standard statistical thermodynamic methods[42] using the unscaled B3LYP frequencies.

The B3LYP/6-311G(d) level of theory proved to be the best compromise between computational cost and accuracy. This paper studies systems of up to eight heavy atoms, which is too costly for high-accuracy methods, such as the G2 approach. However, preliminary calculations for our previous paper[26] indicate that energies obtained using the B3LYP/6-311G(d) level approximate G2 energies for the titanium compounds we studied which contain chloro, nitrido, amido, and imido ligands.

(19) Baboul, A. G.; Schlegel, H. B. *J. Phys. Chem. B* **1998**, *102*, 5152.
(20) Hildenbrand, D. L. *High. Temp. Mater. Sci.* **1996**, *35*, 151.
(21) Everhart, J. B.; Ault, B. S. *Inorg. Chem.* **1995**, *34*, 4379.
(22) Winter, C. H.; Lewkebandara, T. S.; Sheridan, P. H.; Proscia, J. W. *Mater. Res. Soc. Symp. Proc.* **1993**, *282*, 293.
(23) Winter, C. H.; Lewkebandara, T. S.; Proscia, J. W.; Rheingold, A. L. *Inorg. Chem.* **1994**, *33*, 1227.
(24) Siodmiak, M.; Frenking, G.; Korkin, A. *J. Mol. Model.* **2000**, *6*, 413.
(25) Allendorf, M. D.; Janssen, C. L.; Colvin, M. E.; Melius, C. F.; Nielsen, I. M. B.; Osterheld, T. H.; Ho, P. *Proc. Electrochem. Soc.* **1995**, *95−2*, 393.
(26) Cross, J. B.; Schlegel, H. B. *Chem. Mater.* **2000**, *12*, 2466.
(27) Bradley, D. C.; Torrible, E. G. *Can. J. Chem.* **1963**, *41*, 134.
(28) Nugent, W. A.; Harlow, R. L. *Inorg. Chem.* **1979**, *18*, 2030.
(29) Gross, M. E.; Siegrist, T. *Inorg. Chem.* **1992**, *31*, 4898.
(30) Winter, C. H.; Sheridan, P. H.; Lewkebandara, T. S.; Heeg, M. J.; Proscia, J. W. *J. Am. Chem. Soc.* **1992**, *114*, 1095.
(31) Fix, R. M.; Gordon, R. G.; Hoffman, D. M. *Chem. Mater.* **1990**, *2*, 235.
(32) Frisch, M. J.; Trucks, G. W.; Schlegel, H. B.; Scuseria, G. E.; Robb, M. A.; Cheeseman, J. R.; Zakrzewski, V. G.; Montgomery, J. A.; Stratmann, R. E.; Burant, J. C.; Dapprich, S.; Millam, J. M.; Daniels, A. D.; Kudin, K. N.; Strain, M. C.; Farkas, O.; Tomasi, J.; Barone, V.; Cossi, M.; Cammi, R.; Mennucci, B.; Pomelli, C.; Adamo, C.; Clifford, S.; Ochterski, J.; Petersson, G. A.; Ayala, P. Y.; Cui, Q.; Morokuma, K.; Malick, D. K.; Rabuck, A. D.; Raghavachari, K.; Foresman, J. B.; Cioslowki, J.; Ortiz, J. V.; Stefanov, B. B.; Liu, G.; Liashenko, A.; Piskorz, P.; Komaromi, I.; Gomperts, R.; Martin, R. L.; Fox, D. J.; Keith, T.; Al-Laham, M. A.; Peng, C. Y.; Nanayakkara, A.; Gonzalez, C.; Challacombe, M.; Gill, P. M. W.; Johnson, B. G.; Chen, W.; Wong, M. W.; L Andres, J.; Head-Gordon, M.; Replogle, E. S.; Pople, J. A. *GAUSSIAN 98*; Gaussian, Inc.: Pittsburgh, PA, 1998.
(33) Becke, A. D. *Phys. Rev. A* **1988**, *38*, 3098.
(34) Becke, A. D. *J. Chem. Phys.* **1993**, *98*, 5648.
(35) Lee, C.; Yang, W.; Parr, R. D. *Phys. Rev. B* **1988**, *37*, 785.
(36) Krishnan, R.; Binkley, J. S.; Seeger, R.; Pople, J. A. *J. Chem. Phys.* **1980**, *72*, 650.
(37) McLean, A. D.; Chandler, G. S. *J. Chem. Phys.* **1980**, *72*, 5639.
(38) Wachters, A. J. H. *J. Chem. Phys.* **1970**, *52*, 1033.
(39) Hay, J. P. *J. Chem. Phys.* **1977**, *66*, 4377.
(40) Raghavachari, K.; Trucks, G. W. *J. Chem. Phys.* **1989**, *91*, 1062.
(41) Scott, A. P.; Radom, L. *J. Phys. Chem.* **1996**, *100*, 16502.
(42) McQuarrie, D. A. *Statistical Thermodynamics*; University Science Books: Mill Valley, CA, 1973.

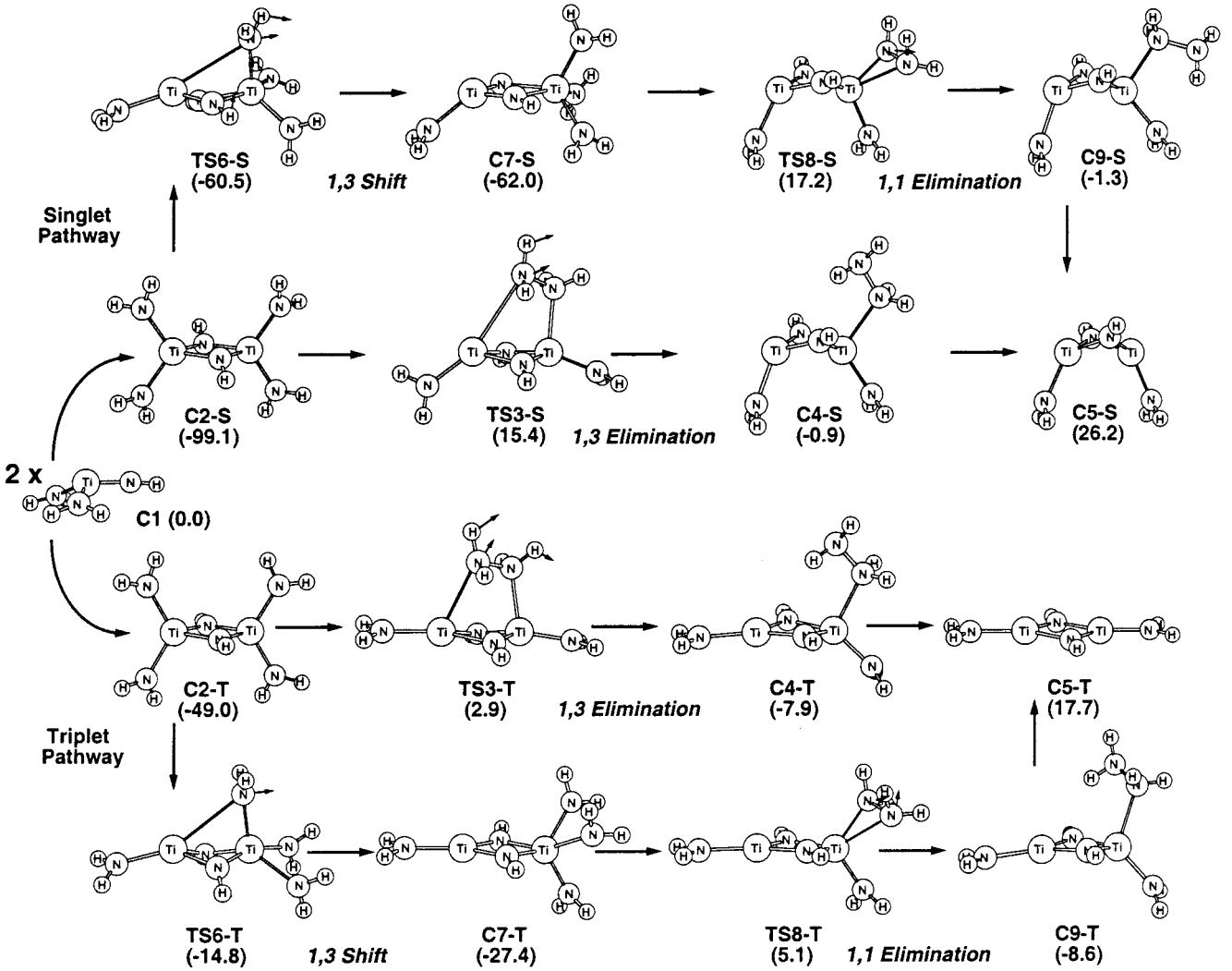

Figure 1. Structures on the singlet and triplet 1,3 elimination and 1,3 shift + 1,1 elimination reaction paths, including molecules and complexes (denoted by C), and transition states with transition vectors (denoted by TS). Singlet structures are designated by a suffix of S and triplet structures by T. Relative enthalpies at 0 K in kcal/mol are included in parentheses.

[For $Ti(NH_2)_4 \rightarrow Ti(NH_2)_2NH + NH_3$ the heats of reaction are 46.4 and 52.5 kcal/mol, and the transition state barriers are 33.5 and 38.4 kcal/mol for the G2 and B3LYP/6-311G(d) levels of theory, respectively.] Activation energies for $Ti(NR_2)_4 + NH_3 \rightarrow Ti(NR_2)_3NH_2 + HNR_2$ measured experimentally[43−45] at 8 and 12 kcal/mol for R = Me and Et, respectively, compare favorably to a barrier height of 9 kcal/mol for the B3LYP/6-311G(d) level of theory. For a more complete discussion supporting this choice of level of theory, see the Methods section of our previous paper.[26]

Results and Discussion

Imido dimerization can be followed by either (a) 1,3 elimination of N_2H_4 or (b) 1,3 shift of NH_2 plus 1,1 elimination of N_2H_4, and each reaction path can proceed on a singlet or triplet surface. Transition state structures are labeled with TS, and complexes representing minima are labeled with C; singlet structures are indicated by a suffix of -S and triplet structures by -T.

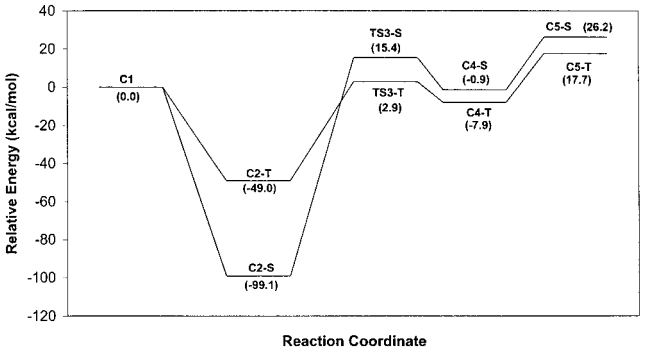

Figure 2. Energy profile for the 1,3 elimination reaction paths. Relative enthalpies at 0 K in kcal/mol are included in parentheses.

Structures along these four reaction paths are shown in Figure 1. Relative energies for the dimerization + 1,3 elimination reaction path are plotted in Figure 2. Relative energies for the dimerization + 1,3 shift + 1,1 elimination reaction path are plotted in Figure 3. During the investigation of these paths, we came across the ring exchange reaction paths shown in Figure 4. Computed heats of formation, entropies, relative enthalpies, and free energies are listed in Table 1.

(43) Weiller, B. H. *Chem. Mater.* **1995**, *7*, 1609.
(44) Weiller, B. H. *J. Am. Chem. Soc.* **1996**, *118*, 4975.
(45) Weiller, B. H. *Mater. Res. Soc. Symp. Proc. USLI* **1996**, *11*, 409.

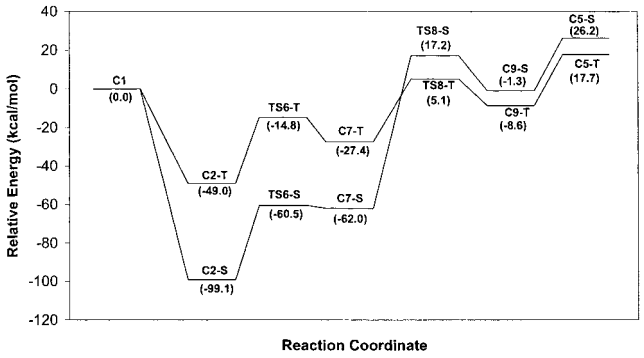

Figure 3. Energy profile for the 1,3 shift + 1,1 elimination reaction paths. Relative enthalpies at 0 K in kcal/mol are included in parentheses.

Table 1. Heats of Formation, Absolute Entropies, Relative Enthalpies, and Relative Free Energies

structure	$\Delta H_{f,298}$[a] (kcal/mol)	entropy[b] (cal/(mol K))	rel enthalpy[c] (kcal/mol)	rel free energy[d] (kcal/mol)
2 × **C1**	−20.6	159.0	0.0	0.0
C2-S	−119.2	118.4	−98.6	−73.8
TS3-S	−5.8	110.9	14.8	44.0
C4-S	−21.7	113.5	−1.1	26.6
C5-S + N_2H_4	5.0	150.3	25.6	31.1
TS6-S	−81.4	111.1	−60.8	−32.0
C7-S	−82.4	116.1	−61.8	−35.7
TS8-S	−3.7	112.6	16.9	45.0
C9-S	−22.2	113.9	−1.6	25.9
TS10-S	−96.9	110.0	−76.3	−46.9
C11-S	−105.2	155.5	−84.6	−58.2
2 × **C1**	−20.6	159.0	0.0	0.0
C2-T	−68.5	124.5	−47.9	−26.4
TS3-T	−18.2	113.7	2.4	30.0
C4-T	−28.2	124.5	−7.6	14.3
C5-T + N_2H_4	−2.9	159.1	17.7	18.4
TS6-T	−35.2	118.0	−14.6	10.5
C7-T	−47.5	119.8	−26.9	−2.9
TS8-T	−15.4	118.7	5.2	30.0
C9-T	−29.0	121.0	−8.4	15.3
TS10-T	−56.6	116.6	−36.0	−10.2
C11-T	−63.4	122.4	−42.8	−20.2

[a] Heats of formation at 298.15 K and 1 atm, computed using the relative enthalpies for the above compounds and $Ti(NH_2)_4$, the experimental $\Delta H_{f,298}$ for $TiCl_4$ (−182.4 kcal/mol), NH_3 (−11.0 kcal/mol), and HCl (−22.1 kcal/mol), and the calculated enthalpy for $TiCl_4 + 4NH_3 \rightarrow Ti(NH_2)_4 + 4HCl$ (70.5 kcal/mol). [b] Absolute entropies at 298.15 K and 1 atm. [c] Enthalpies relative to **C1** at 298.15 K and 1 atm. [d] Free energies relative to **C1** at CVD conditions (523.15 K and 20 Torr).

1. Imido Dimer Formation. Our previous work[26] suggests that, in the gas phase, formation of $Ti(NH_2)_2NH$ is the thermodynamically most favorable elimination product starting from $Ti(NH_2)_4$. Experimental evidence indicates that titanium imido complexes can form oligomers in the gas phase,[5] which could lead to further small molecule elimination reactions and a change in oxidation state from Ti(IV) to Ti(III).

The simplest case for this oligomerization process is the formation of a titanium imido dimer from two $Ti(NH_2)_2NH$ molecules. The reaction path optimization method of Ayala and Schlegel[46] was used to probe for a transition state. This method showed that there is no transition structure and that the dimerization reaction is barrierless. The singlet dimer structure (**C2-S**) has a large binding enthalpy and lies 99.1 kcal/mol below $Ti(NH_2)_2NH$ (**C1**) at 0 K as illustrated in Figure 2. This complex contains a planar Ti_2N_2 ring in which all four Ti−N bonds are 1.912 Å in length and the two imido hydrogens lie out of the plane in a trans conformation with an N−H bond length of 1.018 Å. The remaining $Ti-NH_2$ bonds are all 1.908 Å, giving the molecule C_{2h} symmetry. The triplet dimer structure (**C2-T**) has a much smaller binding enthalpy relative to $Ti(NH_2)_2NH$ (**C1**), 49.0 kcal/mol, and is 50.1 kcal/mol above the singlet complex. **C2-T** also contains a planar Ti_2N_2 ring, but the Ti−N bond lengths are not all equal. The two Ti−N bonds to one of the ring nitrogen atoms are 2.004 Å, while the Ti−N bonds to the other nitrogen are 1.910 Å. In this structure, the imido hydrogen atoms lie in the plane of the ring, and the N−H bond length is 1.017 Å. All four of the $Ti-NH_2$ bonds are 1.931 Å long, resulting in C_{2v} symmetry for the molecule. Inspection of the molecular orbitals reveals that the unpaired electrons are localized on the titanium atoms and amido ligands with no density on the imido groups in the ring.

2. 1,3 Elimination Pathway. To proceed from the dimer complexes through hydrazine elimination, there are two important reaction pathways to explore. The first reaction path involves the 1,3 elimination of amido ligands from the dimer yielding hydrazine (N_2H_4) and $[Ti(\mu\text{-}NH)(NH_2)]_2$ as products. Once again, it is necessary to explore both the singlet and triplet reaction paths to fully understand the energetics involved in this reaction.

The singlet pathway is highly endothermic, 125.3 kcal/mol from the dimer complex (**C2-S**), but only 26.2 kcal/mol from the reactant structure (**C1**), as illustrated in Figure 2. The product structure (**C5-S**) belongs to the C_{2v} point group and is quite different from the dimer structure. Instead of the planar ring of the dimer, the product Ti_2N_2 ring has assumed a symmetrical bent conformation with all Ti−N bonds 1.908 Å long. The angle between the two N−Ti−N planes in the ring is 30.5°. The imido N−H bonds are 1.017 Å and are in a cis conformation. The amido ligands have $Ti-NH_2$ bond lengths of 1.933 Å, and the Ti−Ti−NH_2 angle is 115.8°. Examination of the molecular orbitals reveals the reason for the geometry of this complex. There are large lobes of electron density on the side of the ring opposite to the amido ligands that appear to be the d_{z^2} orbitals of the titanium atoms. The transition state (**TS3-S**) lies 114.5 kcal/mol above the singlet dimer complex (or 15.4 kcal/mol above the reactant (**C1**) compound). The geometry of **TS3-S** shows that one of the amido ligands has migrated all the way across the ring structure and formed a bond with an amido group bound to the other titanium atom (the H_2N-NH_2 bond length is 1.440 Å). The resulting hydrazine group is still bound to the four-member ring, but the Ti−N bond length has increased from 1.908 Å in the dimer to 2.215 Å in the transition state. Accompanying these prominent geometry changes are some subtle distortions in the Ti_2N_2 ring which break the symmetry observed in the dimer, as well as some motion of the remaining amido groups (with lengthening of one $Ti-NH_2$ bond to 1.958 Å). This is a late transition state closely resembling the post-transition-state complex (**C4-S**), which is expected for such an endothermic reaction. This complex (**C4-S**) is 16.3 kcal/mol lower than the transition state (**TS3-S**) and 0.9

(46) Ayala, P. Y.; Schlegel, H. B. *J. Chem. Phys.* **1997**, *107*, 375.

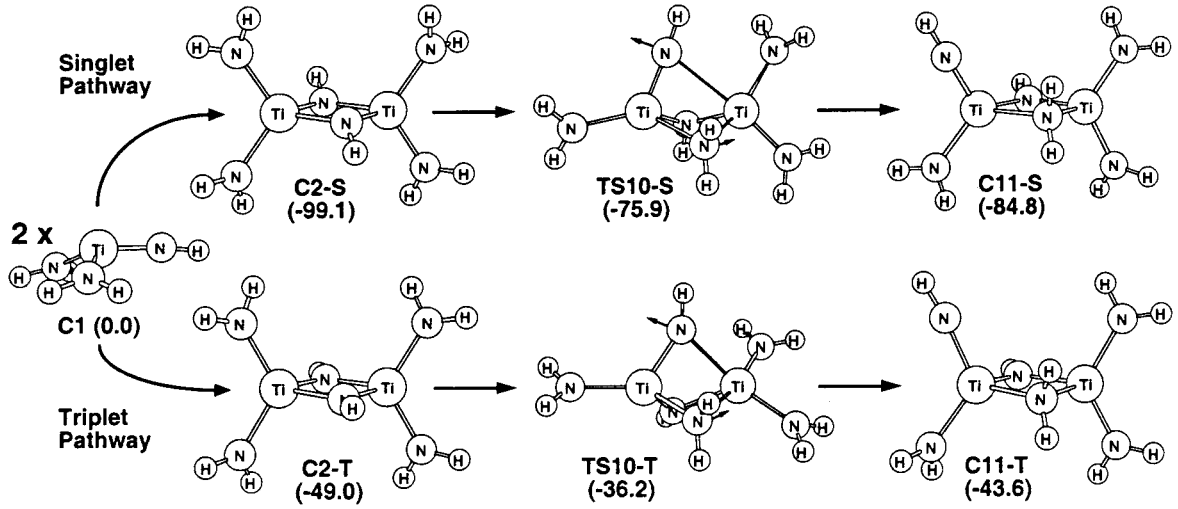

Figure 4. Structures on the singlet and triplet ring exchange reaction paths, including molecules and complexes (denoted by C), and transition states with transition vectors (denoted by TS). Singlet structures are designated by a suffix of S and triplet structures by T. Relative enthalpies at 0 K in kcal/mol are included in parentheses.

kcal/mol below reactants (**C1**). The hydrazine binding energy for this state is 27.1 kcal/mol. The major structural difference from the transition state is that the hydrazine ligand is completely formed and is in the low-energy, gauche conformation; the position of the remaining amido ligands is comparable to that in the product structure (**C5-S**).

The triplet pathway is less endothermic; the products are 17.7 kcal/mol above the reactant structure (**C1**), and 66.7 kcal/mol separates the dimer and products (Figure 2). The product structure (**C5-T**) is completely planar with D_{2h} symmetry. The four Ti−N bonds in the ring are each 1.920 Å, and the imido N−H bonds are 1.016 Å long. The unpaired electrons are located on the amido ligands, but unlike the dimer (**C2-T**) there is a small amount of spin density on the imido groups in the ring. The highest doubly occupied molecular orbitals show extensive conjugation in the ring but no density on the amido ligands. The amido Ti−NH_2 bond lengths have remained almost identical to those in the dimer at 1.934 Å. The transition state (**TS3-T**) can again be classified as late, though it is not as far along the reaction path as in the singlet case. (This is expected since the triplet pathway is much less endothermic than the corresponding singlet pathway.) **TS3-T** lies 51.9 kcal/mol above the dimer complex (**C2-T**) and 2.9 kcal/mol above the reactant structure (**C1**). The central Ti−N ring is very slightly bent, and the Ti−N bonds are no longer symmetric. The bond between the amido groups being eliminated as hydrazine is almost completely formed (1.443 Å), and the Ti−N_2H_4 bond length has elongated from 1.931 Å in the dimer to 2.242 Å. The remaining Ti−NH_2 bonds have assumed a nearly planar conformation with respect to the ring and have lengthened to 1.953 and 1.965 Å. The post-transition-state complex (**C4-T**) lies 41.1 kcal/mol above the dimer (**C2-T**) and 7.9 kcal/mol below the reactant (**C1**). The hydrazine binding energy for this structure is 25.6 kcal/mol. The geometry is very close to that of the transition state (**TS3-T**) with the hydrazine ligand fully formed and in the gauche conformation.

3. 1,3 Shift Followed by 1,1 Elimination Pathway. The second important reaction path involves a two-step reaction; the 1,3 shift of one amido ligand followed by 1,1 elimination of hydrazine from the dimer structure. Both the singlet and triplet pathways have the same reactant (**C2-S**, **C2-T**) and product (**C5-S**, **C5-T**) structures as in the 1,3 elimination pathways described above.

The 1,3 shift singlet transition state (**TS6-S**) lies 38.6 kcal/mol above the dimer complex (**C2-S**), and the amido shift is nearly complete. In the transition state, the Ti−NH_2 bond that is forming with the shifting amido ligand has a length of 1.944 Å, and the Ti−NH_2 bond that is breaking has lengthened to 3.141 Å. The Ti_2N_2 ring has assumed a slight bent conformation, and one of the ring Ti−N bonds to the titanium accepting the third amido ligand has elongated to 2.372 Å; inspection of the molecular orbitals shows electron density from this imido nitrogen localized between itself and the titanium. The combination of these characteristics suggests that it is now a dative bond. The subsequent complex (**C7-S**) is one in which the ligand migration is complete. This complex is only 1.5 kcal/mol below the transition state (**TS6-S**) and 37.1 kcal/mol above the dimer complex (**C2-S**). The Ti_2N_2 ring has returned to a planar conformation and still exhibits a Ti−N bond length indicative of a dative bond to the titanium with three amido ligands (bond length of 2.287 Å). The four amido Ti−NH_2 bonds all remain between 1.909 and 1.932 Å. The 1,1 elimination transition state (**TS8-S**) lies 79.2 kcal/mol above the ligand migrated complex (**C7-S**) and 17.2 kcal/mol above the reactant complex (**C1**). The hydrazine N−N bond formation is well underway in the transition state (1.816 Å), and the Ti−NH_2 bond lengths to these two amido ligands have lengthened to 2.059 and 2.393 Å. The remainder of the structure closely resembles the product geometry (**C5-S**). The Ti_2N_2 ring has assumed a bent conformation, and the dative bond that was evident in structures **TS6-S** and **C7-S** has been replaced by a covalent bond (bond length of 1.980 Å). The two remaining amido ligands have Ti−NH_2 bond lengths of 1.936 and 1.940 Å. The post-elimination complex (**C9-S**) lies 60.7 kcal/mol above the ligand migrated complex (**C7-S**), and the hydrazine binding energy is 27.5 kcal/mol. The Ti−N_2H_4 bond has length-

ened to 2.247 Å with the hydrazine ligand in the gauche conformation. The rest of the geometry is essentially the same as the product structure (**C5-S**).

The 1,3 shift triplet transition state (**TS6-T**) lies 34.2 kcal/mol above the dimer complex (**C2-T**) and shows nearly completed ligand migration. The Ti−NH_2 bond that is forming with the shifting amido ligand has a length of 1.935 Å, and the Ti−NH_2 bond that is breaking has lengthened to 3.141 Å. The Ti_2N_2 ring is slightly distorted from the planar conformation, and the two original amido ligands that remain bonded to the titanium coordinated to a third amido group have lengthened Ti−NH_2 bonds (2.091 and 2.131 Å). The ligand migrated complex (**C7-T**) is 12.6 kcal/mol below the transition state (**TS6-T**) and 21.6 kcal/mol above the dimer complex (**C2-T**). The ring has returned to a planar conformation, and two of the amido ligands bonded to the higher coordinated titanium have elongated Ti−NH_2 bonds (2.054 and 2.125 Å compared to 1.931 Å in the dimer **C2-T**). The 1,1 elimination triplet transition state (**TS8-T**) lies 32.5 kcal/mol above the ligand migrated structure (**C7-T**) and 54.1 kcal/mol above the dimer complex (**C2-T**). The hydrazine N−N bond is partially formed (1.723 Å), and the ligands forming the hydrazine have Ti−N bond lengths of 2.085 and 2.395 Å. The Ti_2N_2 ring has remained planar, along with the lone amido ligand attached to one of the titanium atoms. The post-elimination complex (**C9-T**) lies 18.8 kcal/mol above the ligand migrated complex (**C7-T**), and the hydrazine binding energy is 26.3 kcal/mol. The hydrazine N−N bond is completely formed (1.449 Å) in the gauche conformation, and the Ti−N_2H_4 bond has lengthened to 2.255 Å. The Ti−N ring, along with one amido ligand, is planar with only one of the remaining amido ligands out of the plane.

4. Ring Exchange Reactions. The elimination reaction paths outlined above are not the only feasible reactions from the imido dimer structures (**C2-S**, **C2-T**). During the investigation of these reactions, several structures were found that belong to a ring exchange reaction path, in which an amido group replaces an imido group in the four-membered ring.

The singlet pathway leading to single amido-imido exchange in the ring is endothermic by 14.3 kcal/mol relative to the dimer structure (**C2-S**). The transition state barrier is 23.2 kcal/mol, and the geometry is roughly halfway between the reactant structure (**C2-S**) and product structure (**C11-S**) with the ring in a bent conformation. The amido group has already formed the bonds that make it part of the ring (Ti−NH_2 bond lengths of 2.132 and 2.130 Å), while the imido group leaving the ring has one Ti−NH bond shortened to 1.706 Å (compared to 1.912 in the dimer) and the other lengthened to 2.726 Å. The ring exchange complex (**C11-S**) once again has a planar four-member ring and superficially resembles the **C2-S** dimer structure but has several structural differences and lacks the symmetry present in that structure. The Ti−NH bond to the imido ligand no longer in the ring has shortened to 1.684 Å, and the Ti−NH bonds to the ring imido group have changed to 2.059 and 1.814 Å from 1.912 Å in the dimer complex (**C2-S**). This structure could be on the pathway for forming higher oligomers.

The triplet pathway leading to amido−imido ring exchange is endothermic by 5.4 kcal/mol and has a transition state barrier of 12.8 kcal/mol. The transition state geometry has a bent ring and is midway between reactants (**C2-T**) and products (**C11-T**) but is not quite as far along the reaction path as in the singlet case (**TS10-S**). The amido ligand is bonded to both titanium atoms (bond lengths of 1.995 and 2.407 Å), and the imido group leaving the ring has a Ti−NH bond lengthened to 2.232 Å while the other has shortened to 1.845 Å. The ring exchange complex (**C11-T**) is planar and closely resembles the dimer complex (**C2-T**); however, there are a number of geometric differences within the ring section that break the symmetry found in **C2-T**. The amido ligand in the ring has Ti−NH_2 bond lengths of 2.061 and 2.151 Å, and the Ti−NH bond lengths to the imido ligand in the ring have distorted to 1.844 and 1.987 Å. The imido ligand outside of the ring has a Ti−NH bond length of 1.875 Å, which is slightly longer than in the transition state (**TS10-T**).

Conclusions

A simple inspection of Figures 2 and 3 shows that crossing from the singlet to triplet states occurs along both of these reaction paths. The crossing occurs between the imido dimer complex (**C2-S**) and the 1,3 elimination transition state (**TS3-T**) for the 1,3 elimination pathway and between the ligand migrated complex (**C7-S**) and 1,1 elimination transition state (**TS8-T**) for the 1,3 shift + 1,1 elimination pathway. It is well-known that, for heavy elements such as Ti, singlet to triplet crossing occurs readily and that the time scale for these crossings is much shorter than the time scale for the reaction.

Although both the singlet and triplet reactions are endothermic (by 26.2 and 17.7 kcal/mol, respectively), the large binding enthalpies of the dimer structures (**C2-S** at 99.1 kcal/mol and **C2-T** at 49.0 kcal/mol) are the dominant features of the energy profiles. Inspection of the reaction free energies shows that there is little qualitative difference from the reaction enthalpies, suggesting that the thermodynamics of these reactions is controlled by enthalpic contributions and that entropic factors are of little importance in the overall reaction. These factors indicate that the oligomer imido complex (modeled by the dimer complex in this work) postulated by Dubois[5] is very stable and is likely to be the compound that interacts with the titanium nitride surface during CVD. Subsequent elimination of N_2H_4 is rather endothermic relative to the dimer complex, suggesting that reduction of Ti(IV) to Ti(III) may occur on the surface rather than in the gas phase.

Acknowledgment. We gratefully acknowledge support from the National Science Foundation (CHE 98-74005) and from the National Computational Science Alliance under CHE980042N utilizing the NCSA HP/Convex Exemplar SPP-2200.

Supporting Information Available: Tables of total energies, Cartesian coordinates, and vibrational frequencies of the structures described in this work (PDF). This material is available free of charge via the Internet at http://pubs.acs.org.

CM000840C